PHYSICAL REVIEW A VOLUME 47, NUMBER 1 JANUARY 1993

Self-consistent calculations of atomic properties using self-interaction-free exchange-only Kohn-Sham potentials

Yan Li and J. B. Krieger
Department of Physics, Brooklyn College, City University of New York, Brooklyn, New York 11210

G. J. Iafrate
U.S. Army Research Office, Research Triangle Park, North Carolina 27709-2211

(Received 1 May 1992)

The spin-unrestricted optimized-effective-potential (OEP) method and an approximation to it due to the authors (KLI) have been applied to atoms from Li ($Z=3$) to Ba ($Z=56$) plus Au ($Z=79$) and Hg ($Z=80$) within the exchange-only scheme. Calculations were performed for the term with the lowest energy in the ground-state configuration. For a few transition elements, terms in the low-lying excited-energy-state configuration are also self-consistently calculated. We have compared our OEP and KLI results with each other and with those obtained from the spin-unrestricted Hartree-Fock (SUHF) method and the local-spin-density exchange-only (LSDX) approximation. As the spin-restricted OEP, the spin-unrestricted OEP yields nearly identical results as the corresponding SUHF. The relative difference of the total energy from that of the SUHF is only 40 ppm for ^{3}Li and monotonically decreases as Z increases to less than 2 ppm for ^{80}Hg. The highest occupied energy eigenvalues of each spin projection, $\varepsilon_{m\sigma}$, and the various expectation values for the operators r^2, r^{-1}, and $\delta(\mathbf{r})$ are all very similar to the SUHF theory. For most of the atoms, even the spin density mimics the SUHF value quite well. Differences appear to be larger for some transition- and noble-metal atoms. Nevertheless, even in these cases, the total energy and the total electron density of the OEP calculations are still very similar to the corresponding SUHF values. For atoms with the highest occupied energy eigenvalues having the same spatial quantum numbers for both spin projections, the spin splitting, $\varepsilon_{m\downarrow}-\varepsilon_{m\uparrow}$, corresponding to the difference between the highest occupied eigenvalues of the minority ($\downarrow$) and majority ($\uparrow$) spin states, is also studied. It is found that the OEP and SUHF spin splittings are nearly identical for atoms with the highest occupied eigenstate being a p state. Noticeable differences (of the OEP and HF spin splitting) occur for a few transition elements having an empty $(n-1)d\downarrow$ subshell. However, such larger differences are steadily diminished as the $(n-1)d\downarrow$ subshell is progressively filled. As an approximate Kohn-Sham (KS) potential, the KLI method shows itself to be a much improved one compared to the LSDX. The exchange potential constructed from this method retains many of the essential properties of the exact OEP that the LSDX approximation lacks and thus always yields better densities, lower total energies, and more accurate eigenvalues for the highest occupied energy state of each spin projection than the LSDX approximation. In particular, the total energies overestimate the OEP results by only 9 ppm for Li, with the overestimate decreasing for increasing atomic number Z to less than 1 ppm for $Z>50$. In addition, for atoms other than transition elements or noble metals, the $\varepsilon_{m\sigma}$ are within 0.4% of the corresponding OEP results with slightly larger differences for the other atoms. In all cases, the KLI results for the expectation values r^2, r^{-1} and the density at the origin are very close to the exact KS results and are a significant improvement over those provided by the LSDX approximation.

PACS number(s): 31.10.+z, 31.20.Sy, 31.90.+s, 31.20.Di

I. INTRODUCTION

The central problem of implementing the Kohn-Sham (KS) [1] formalism in calculating the ground-state properties of a many-electron system is to find an accurate approximation to the exchange-correlation potential, $V_{\mathrm{xc}\sigma}(\mathbf{r})$ (where σ denotes spin orientation), which is the functional derivative of the exchange-correlation energy functional $E_{\mathrm{xc}}[n_\uparrow,n_\downarrow]$ with respect to the spin density, $n_\sigma(\mathbf{r})$, since the KS theory, though exact in principle, does not provide a prescription for the exact $V_{\mathrm{xc}\sigma}(\mathbf{r})$ except in the limit of slowly varying density.

Although still unknown, it has nevertheless been shown that the exact $V_{\mathrm{xc}\sigma}(\mathbf{r})$ is characterized by some essential properties. It should be self-interaction free [2] (an electron should not interact with itself via the Coulomb potential); it should have the correct asymptotic structure [assumes the expression of the local-spin-density (LSD) approximation in the uniform-density limit [1,3] and for systems with a finite number of electrons $\rightarrow -1/r$ as r approaches infinity]; it should yield an energy eigenvalue for the highest occupied single-particle state that is exactly equal to the negative of the removal energy [4]; it should exhibit an integer discontinuity [5,6], i.e., when the number of electrons of a system having discrete energy spectrum with filled subshells changes from N to $N+\delta$ (with δ being an infinitesimal), the $V_{\mathrm{xc}\sigma}^{N+\delta}(\mathbf{r})$ will shift from $V_{\mathrm{xc}\sigma}^{N}(\mathbf{r})$ by a constant for finite r.

The currently widely used local-spin-density approximation, $V_{xc\sigma}^{LSD}(\mathbf{r})$, although quite successful in explaining a variety of physical phenomena, fails to qualify as an accurate approximation to the $V_{xc\sigma}(\mathbf{r})$ for any real systems like atoms, molecules, and solids, since it possesses none of the properties mentioned above.

The self-interaction corrected LSD (SICLSD) [2], although possessing many of these important properties, does not lie within the KS framework, since it requires different potentials for each orbital. In addition, because of the fact that multipotentials are employed in the calculation, the SICLSD wave functions are not orthogonal unless off-diagonal Lagrange multipliers are introduced. In this case, however, the amount of time required in the computation will be significantly increased.

In an exchange-only KS theory, in which the exchange energy functional assumes the same form as that of Hartree-Fock (HF) theory:

$$E_x^{HF}[\phi_{i\sigma}]=-\frac{1}{2}\sum_{ij\sigma}\int\frac{\phi_{i\sigma}^*(\mathbf{r})\phi_{i\sigma}(\mathbf{r}')\phi_{j\sigma}^*(\mathbf{r}')\phi_{j\sigma}(\mathbf{r})}{|\mathbf{r}-\mathbf{r}'|}d\mathbf{r}\,d\mathbf{r}' \tag{1}$$

with the $\phi_{i\sigma}$ being the KS orbitals, the $V_{x\sigma}(\mathbf{r})$ can actually be found numerically by employing the optimized-effective-potential (OEP) method [7–9]. One of the advantages of the KS formalism over that of HF is obviously that the former requires only one potential (or two for a spin-polarized system); therefore, all the orbitals are automatically orthogonal. The HF method, like the SICLSD, employs multipotentials, so for most electron systems, it is necessary to introduce off-diagonal Lagrange multipliers in order to have a set of orthogonal orbitals.

Nevertheless, the method of using the OEP to obtain $V_{x\sigma}(\mathbf{r})$ is not without problems. Since in solving the OEP integral equation, one has to invert a matrix of considerable order to achieve reasonable accuracy, a large amount of computer time is consumed. Our experience shows that in a single-term atomic calculation, it actually takes an even longer time to solve the OEP equation than to solve the HF equation, with the accuracy of the numerical OEP solutions being best described as moderate: Virial theorem satisfied to 5–6 digits as compared to the 8–9 digits for the HF solution. For systems like molecules, one will encounter considerable difficulties when employing the OEP, because no method has yet been developed to invert the OEP equation for a nonspherically symmetric system. For these systems, it appears that the most practical approach to proceed is to find an approximate $V_{x\sigma}(\mathbf{r})$ which retains the essential properties of the OEP and is easy to use.

In recent work [10–13], the authors proposed an approximate method of solving the OEP integral equation. An accurate $V_{xc\sigma}(\mathbf{r})$ can be obtained without having to solve the integral equation. Rather, only a set of linear equations of the order equal to the number of nondegenerate orbitals need to be solved. Application to selected atoms [the ten atoms with complete subshells (Be to Xe) and the alkali metals] [10–12] and negative ions (the alkali metals, halogens, and those with incomplete $2p$ and $3p$ subshells) [13] in the exchange-only approximation shows that this method (we will denote it as the KLI method hereafter), yields results that are nearly identical to those of the OEP. The total energies thus obtained are always closer to those of the HF or OEP method than any other density-functional approximations, including the method proposed recently by Harbola and Sahni [14]. For solids with large energy gaps, the band gaps obtained from using this method [15] rectify the familiar large errors of the LSD results [16,17] and agree fairly well with the experimental results [18,19]. Moreover, the exchange potential from this construction maintains nearly all the important properties of the exact OEP: It is self-interaction free, reduces to LSD in the uniform density limit, approaches $-1/r$ as $r\rightarrow\infty$, yields eigenvalues of the highest occupied state that satisfies Koopmans's theorem [20], and exhibits the property of integer discontinuity [12].

Here, we will extend our work to atoms with incomplete subshells using the spin-unrestricted KLI construction. To make a comparison, we will also present the results obtained from using the spin-unrestricted OEP, HF (SUHF), and LSDX formalisms. Our calculations are for atoms from $Z=3$ to $Z=56$ plus two selected atoms with $Z>56$: Au($Z=79$), which completes the set of noble-metal group, and Hg($Z=80$), which is an atom with complete subshells. [The HF, OEP, and KLI methods give identical results for He($Z=2$) and are not displayed]. Calculations are performed for the term with the lowest energy in the ground-state configuration. For a few transition elements, terms in the low-lying excited-energy-state configurations are also self-consistently computed.

Our OEP results are obtained from a modified code of Talman [21]. The total energies reported here are all deeper or equally as low as those previously published [8,22,23]. The condition [24] that $\varepsilon_m=\bar{\varepsilon}_m^{HF}$, where $\bar{\varepsilon}_m^{HF}$ is the expectation value of the single-particle HF Hamiltonian corresponding to the highest-energy occupied state, is always more accurately satisfied. In fact, in most cases, the ε_m and $\bar{\varepsilon}_m^{HF}$ are different by only a few tenths of a millirydberg. The Virial theorem is satisfied to at least five significant digits, and the Virial theorem related identity for the exchange energy $E_x[n_\uparrow,n_\downarrow]$ and the KS exchange potential $V_x(\mathbf{r})$ due to Levy and Perdew [25] is satisfied to four or more digits. Thus, we believe these are more accurate OEP calculations than those previously published.

II. FORMALISM

A. The optimized-effective-potential method

Although the original derivation of the OEP formalism was published nearly 40 years ago [7] and the first numerical calculations were performed more than a decade ago [8], the OEP method, we believe, is still far less familiar to most workers in the field than is the HF or LSD. So, for clarity of the presentation, we briefly review the OEP method, extended here to the spin-unrestricted case.

Consider an expression for the total energy of an electron system with external potential $v_{ext\sigma}(\mathbf{r})$ as a functional of a set of orbitals $\{\phi_{i\sigma}\}$ (where σ denotes the spin orientation and i represents the remaining quantum numbers):

$$E=E[\phi_{i\sigma}]=T[\phi_{i\sigma}]+E_H[n]+E_{\mathrm{xc}}[\phi_{i\sigma}] +\sum_{\sigma}\int d\mathbf{r}\, v_{\mathrm{ext}\sigma}(\mathbf{r})n_\sigma(\mathbf{r}) , \tag{2}$$

where

$$T[\phi_{i\sigma}]=\sum_{i,\sigma}\langle\phi_{i\sigma}|-\tfrac{1}{2}\nabla^2|\phi_{i\sigma}\rangle ,$$

$$E_H[n]=\tfrac{1}{2}\int d\mathbf{r}\,d\mathbf{r}'\frac{n(\mathbf{r}')n(\mathbf{r})}{|\mathbf{r}-\mathbf{r}'|} ,$$

and $E_{\mathrm{xc}}[\phi_{i\sigma}]$ is an approximate expression for the exchange-correlation energy. It can be LSD or SICLSD, or exchange-only HF, $E_{\mathrm{x}}^{\mathrm{HF}}[\phi_{i\sigma}]$ of Eq. (1), etc. The OEP method corresponds to finding the minimum value of $E[\phi_{i\sigma}]$ with the $\{\phi_{i\sigma}\}$ being obtained from a pair of local potentials (for two spin orientations):

$$h_\sigma^{\mathrm{OEP}}\phi_{i\sigma}=(-\tfrac{1}{2}\nabla^2+V_\sigma^{\mathrm{OEP}})\phi_{i\sigma}=\varepsilon_{i\sigma}\phi_{i\sigma} , \tag{3}$$

where the effective potentials V_σ^{OEP} are determined by applying the variational principle to $E[\phi_{i\sigma}]$, i.e.,

$$\frac{\delta E}{\delta V_\sigma}=\sum_i\int\frac{\delta E}{\delta\phi_{i\sigma}^*(\mathbf{r}')}\frac{\delta\phi_{i\sigma}^*(\mathbf{r}')}{\delta V_\sigma(\mathbf{r})}d\mathbf{r}'+\mathrm{c.c.}=0 . \tag{4}$$

Here

$$\frac{\delta\phi_{i\sigma}^*(\mathbf{r}')}{\delta V_\sigma(\mathbf{r})}=-G_{i\sigma}(\mathbf{r}',\mathbf{r})\phi_{i\sigma}(\mathbf{r}) ,$$

$$G_{i\sigma}(\mathbf{r}',\mathbf{r})=\sum_j{}'\frac{\phi_{j\sigma}^*(\mathbf{r}')\phi_{j\sigma}(\mathbf{r})}{\varepsilon_{j\sigma}-\varepsilon_{i\sigma}}$$

(where the prime in the sum indicates that only states with $\varepsilon_{j\sigma}\neq\varepsilon_{i\sigma}$ are summed). So

$$(h_\sigma^{\mathrm{OEP}}-\varepsilon_{i\sigma})G_{i\sigma}(\mathbf{r},\mathbf{r}')=\delta(\mathbf{r}-\mathbf{r}')-\phi_{i\sigma}(\mathbf{r})\phi_{i\sigma}^*(\mathbf{r}') . \tag{5}$$

If we define $h_{i\sigma}$ by

$$\frac{\delta E}{\delta\phi_{i\sigma}^*(\mathbf{r})}=h_{i\sigma}\phi_{i\sigma}(\mathbf{r}) , \tag{6}$$

then

$$h_{i\sigma}=-\tfrac{1}{2}\nabla^2+v_H(\mathbf{r})+v_{\mathrm{ext}\sigma}(\mathbf{r})+v_{\mathrm{xc}i\sigma}(\mathbf{r}) ,$$

where

$$v_{\mathrm{xc}i\sigma}(\mathbf{r})=\frac{\delta E_{\mathrm{xc}}[\phi_{i\sigma}]}{\phi_{i\sigma}\delta\phi_{i\sigma}^*} . \tag{7}$$

If we take $E_{\mathrm{xc}}=E_{\mathrm{x}}^{\mathrm{HF}}$, then the $v_{\mathrm{xc}i\sigma}(\mathbf{r})$ are the usual effective spin-unrestricted HF single-particle potentials. Substituting Eqs. (5), (6), and (7) into (4), the following integral equation for the exchange-correlation potentials,

$$V_{\mathrm{xc}\sigma}(\mathbf{r})\equiv V_\sigma^{\mathrm{OEP}}-\left[v_{\mathrm{ext}\sigma}(\mathbf{r})+\int d\mathbf{r}'\frac{n(r')}{|\mathbf{r}-\mathbf{r}'|}\right] ,$$

is obtained

$$\int H_\sigma(\mathbf{r},\mathbf{r}')V_{\mathrm{xc}\sigma}(\mathbf{r}')d\mathbf{r}'=Q_\sigma(\mathbf{r}) , \tag{8}$$

$$\begin{aligned}H_\sigma(\mathbf{r},\mathbf{r}')&=\sum_i\phi_{i\sigma}^*(\mathbf{r})G_{i\sigma}(\mathbf{r},\mathbf{r}')\phi_{i\sigma}(\mathbf{r}') ,\\ Q_\sigma(\mathbf{r})&=-\sum_i\int d\mathbf{r}'\phi_{i\sigma}^*(\mathbf{r})G_{i\sigma}(\mathbf{r},\mathbf{r}')v_{\mathrm{xc}i\sigma}(\mathbf{r}')\phi_{i\sigma}(\mathbf{r}') .\end{aligned} \tag{9}$$

In this work, since we restrict ourselves in the exchange-only case and treat the exchange exactly, $V_{\mathrm{xc}\sigma}=V_{\mathrm{x}\sigma}$ is the exact KS exchange-only potential [26]. The solution of the OEP equation is then the solution of the integral equation (8) with E_{x} being given by the HF expression, i.e., Eq. (1).

B. An accurate approximate approach to OEP: The KLI method

As described in the Introduction, the major problem with the OEP method is the difficulty one encounters in numerically solving Eq. (8). Even for simple systems like atoms, great effort [27] needs to be taken to ensure that the solution satisfies, to a certain degree of accuracy, some of the exact relations that the OEP obeys. For complex systems like molecules, where the potential lacks spherical symmetry, no systematic method has yet been devised to solve Eq. (8). In the work of KLI [10–12], the OEP integral equation is analyzed and a simple approximation is made which reduces the complexity of the original OEP equation significantly and at the same time keeps many of the essential properties of OEP unchanged. In fact, for a spin-polarized system, an analytic expression similar to the Slater construction for the $V_{\mathrm{xc}\sigma}$, i.e., is obtained:

$$V_{\mathrm{xc}\sigma}(\mathbf{r})=\sum_i\frac{n_{i\sigma}(\mathbf{r})[v_{\mathrm{xc}i\sigma}(\mathbf{r})+(\bar{V}_{\mathrm{xc}i\sigma}-\bar{v}_{\mathrm{xc}i\sigma})]}{n_\sigma(\mathbf{r})} \tag{10}$$

or in a different form

$$V_{\mathrm{xc}\sigma}(\mathbf{r})=V_{\mathrm{xc}\sigma}^S(\mathbf{r})+\sum_i\frac{n_{i\sigma}(\mathbf{r})}{n_\sigma(\mathbf{r})}(\bar{V}_{\mathrm{xc}i\sigma}-\bar{v}_{\mathrm{xc}i\sigma}) , \tag{10'}$$

where

$$V_{\mathrm{xc}\sigma}^S(\mathbf{r})=\sum_i\frac{n_{i\sigma}(\mathbf{r})v_{\mathrm{xc}i\sigma}(\mathbf{r})}{n_\sigma(\mathbf{r})} , \tag{11}$$

which is essentially the exact Slater potential [28] when $E[\phi_{i\sigma}]=E_{\mathrm{HF}}[\phi_{i\sigma}]$. Here $n_{i\sigma}(\mathbf{r})$ is the orbital density, $n_{i\sigma}(\mathbf{r})=|\phi_{i\sigma}(\mathbf{r})|^2$, and $n_\sigma(\mathbf{r})=\sum_i n_{i\sigma}(\mathbf{r})$. $\bar{V}_{\mathrm{xc}i\sigma}$ and $\bar{v}_{\mathrm{xc}i\sigma}$ are the expectation values of $V_{\mathrm{xc}\sigma}(\mathbf{r})$ and $v_{\mathrm{xc}i\sigma}(\mathbf{r})$ with respect to orbital $i\sigma$.

The solution of Eq. (10) or (10′) is unique up to an additive constant as is the case for Eq. (8), which can be determined when one requires that $V_{\mathrm{xc}\sigma}(\mathbf{r})$ goes to zero as r approaches infinity. Then, $\bar{V}_{\mathrm{xc}m\sigma}=\bar{v}_{\mathrm{xc}m\sigma}$ and

$$\varepsilon_{m\sigma}=\bar{\varepsilon}_{m\sigma}\equiv\left\langle\phi_{m\sigma}\left|\frac{\delta E}{\phi_{m\sigma}\delta\phi_{m\sigma}^*}\right|\phi_{m\sigma}\right\rangle \tag{12}$$

is always satisfied [10], which is an exact relationship of the OEP solution [24]. Here $\varepsilon_{m\sigma}$ is the highest occupied single-particle energy eigenvalue. The other $\bar{V}_{\mathrm{xc}i\sigma}$ may be determined by inverting a matrix of the order of the number of nondegenerate orbitals, i.e.,

$$\bar{V}^{i}_{\mathrm{xc}\sigma}=\bar{v}_{\mathrm{xc}i\sigma}+\sum_{j}^{m-1}(A_{\sigma}^{-1})_{ij}(\bar{V}^{S}_{\mathrm{xc}j\sigma}-\bar{v}_{\mathrm{xc}j\sigma}) \qquad (i=1,2,\ldots,m-1)\ , \qquad (13)$$

where

$$(A_{\sigma})_{ji}\equiv\delta_{ji}-(M_{\sigma})_{ji}\ , \qquad (14)$$

with

$$(M_{\sigma})_{ji}\equiv\int d\mathbf{r}\frac{n_{j\sigma}(\mathbf{r})n_{i\sigma}(\mathbf{r})}{n_{\sigma}(\mathbf{r})} \qquad (i,j=1,2,\ldots,m-1)\ . \qquad (15)$$

The difference of this $V_{\mathrm{xc}\sigma}(\mathbf{r})$ from the Slater approximation is entirely due to the second term in Eq. (10′) [or, comparing Eq. (10) with Eq. (11), the difference is that each $v_{\mathrm{xc}i\sigma}(\mathbf{r})$ is shifted by a constant: $\bar{V}_{\mathrm{xc}i\sigma}-\bar{v}_{\mathrm{xc}i\sigma}$]. It is this term which enables the KLI $V_{\mathrm{xc}\sigma}(\mathbf{r})$ to preserve the property of integer discontinuity. The Slater contribution, on the other hand, ensures that this potential goes to $-1/r$ as $r\to\infty$. The condition of $\bar{V}_{\mathrm{xc}m\sigma}=\bar{v}_{\mathrm{xc}m\sigma}$ yields the LSD expression for $V_{\mathrm{xc}\sigma}(\mathbf{r})$ in the uniform-density limit [12].

III. RESULTS AND DISCUSSION

We have performed the spin-unrestricted HF, OEP, KLI, and LSDX calculations for atoms from $Z=3$ to $Z=56$ plus Au($Z=79$) and Hg ($Z=80$). Some results for the ten atoms with complete subshells (Be to Xe) as well as for the alkali metals (Li, Na, and K) have previously been reported by the authors [10–12]. To make our comparisons complete, however, we will include these results in the tables as well.

A. Total energy

The expectation value of a many-electron Hamiltonian with respect to a single Slater determinant (for an open-shell atom, it may require a linear combination of several Slater determinants in order that the total wave function be an eigenfunction of the total orbital and angular momentum operators L^2 and S^2), i.e., the total energy, yields its absolute minimum when the set of single-particle wave functions of the Slater determinants are obtained from solving the HF equations. On the other hand, another minimum value, which lies above that of HF, is obtained from a Slater determinant (or a linear combination of Slater determinants) constructed from a subset of single-particle wave functions constrained to be solutions from a pair of Schrödinger equations with spin-dependent potentials, by employing the OEP method.

It follows that the Slater determinant constructed from any other KS approximations, like KLI or LSDX, will lead to total energy values that are upper bounds to the OEP result. Here we would like to investigate how close this upper bound is to the OEP results when the KLI approximation is applied.

Table I lists the negative values of the total energy in atomic units as obtained from SUHF, OEP, and KLI methods. For a better illustration, we plot the fractional overestimates (for only the ground-state configuration) of the various density functional theory (DFT) calculations from the SUHF values (in ppm) in Fig. 1. The LSDX result is also included in this figure for comparison. It is seen that the curve of the relative errors of the LSDX always lie above that of KLI which only slightly overestimates the OEP results. This indicates that in all cases, the inequality $E_{\mathrm{HF}}<E_{\mathrm{OEP}}<E_{\mathrm{KLI}}<E_{\mathrm{LSDX}}$ is always true. Note that whereas the conditions $E_{\mathrm{HF}}<E_{\mathrm{OEP}}<E_{\mathrm{KLI}}$ and $E_{\mathrm{HF}}<E_{\mathrm{OEP}}<E_{\mathrm{LSDX}}$ are guaranteed by the variational principle, the fact that the inequality $E_{\mathrm{KLI}}<E_{\mathrm{LSDX}}$ is always satisfied indicates that the KLI wave functions are indeed a better approximation to those of the SUHF or OEP than the LSDX solutions. A more careful study of Fig. 1 or Table I shows that the two minima of E_{HF} and E_{OEP} are in fact extremely close: The E_{OEP} are different from E_{HF} by just 40 ppm for Be and the differences decrease to slightly more than 2 ppm for Ba (for Au and Hg, the difference is less than 1.7 ppm). The difference of E_{KLI} and E_{HF} is only about a third larger, i.e., it drops from about 50 ppm for Be to be about 3 ppm for Ba. The E_{KLI} results are in error compared to the E_{OEP} by only about 10 ppm for Be, down to less than 1 ppm for Ba. For Au and Hg, the errors reduce to less than 0.5 ppm. The E_{LSDX}, on the other hand, differs from E_{HF} by nearly 550 ppm for Li, 336 ppm for Be, and 6.5 ppm for Ba. It has errors relative to OEP that are at least a factor of 5 larger than those of KLI. In addition, from Fig. 1, it is seen that even the shape of the OEP and KLI total energy versus atomic number is more like each other than that of LSDX.

Finally, we note that for the atom Zr, an element in the second transition group, the exchange-only calculation predicts a ground-state configuration that is different from that currently known [29]. Instead of $4d^25s^2(^3F)$, term $4d^35s^1(^5F)$ yields a lower total energy.

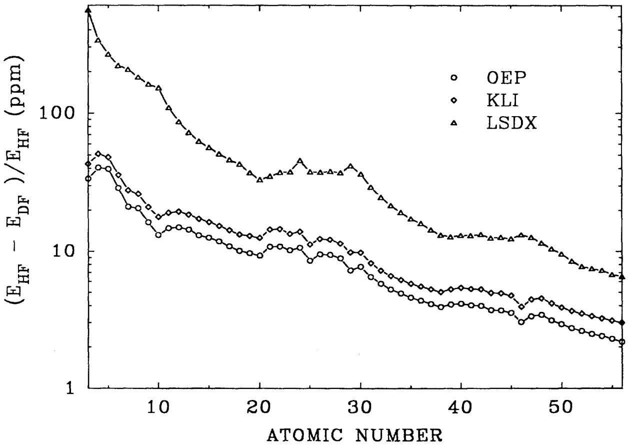

FIG. 1. Fractional overestimates of the OEP, KLI, and LSDX total ground-state energies over that of the SUHF theory.

TABLE I. Total energy of atoms in spin-unrestricted SUHF, OEP, and KLI calculations. Besides ground state, some low-lying excited terms for a few transition- and noble-metal atoms are also presented. Negative values of the energy in atomic units are listed.

Z	Atom	Configuration	Term	SUHF	OEP	KLI
3	Li	$2s^1$	^2S	7.432 75	7.432 50	7.432 43
4	Be	$2s^2$	^1S	14.573 02	14.572 43	14.572 28
5	B	$2p^1$	$^2\mathrm{P}$	24.529 31	24.528 34	24.528 13
6	C	$2p^2$	^3P	37.690 00	37.688 91	37.688 65
7	N	$2p^3$	^4S	54.404 55	54.403 40	54.403 04
8	O	$2p^4$	^3P	74.813 63	74.812 08	74.811 67
9	F	$2p^5$	^2P	99.410 84	99.409 22	99.408 75
10	Ne	$2p^6$	^1S	128.5471	128.5454	128.5448
11	Na	$3s^1$	^2S	161.8590	161.8566	161.8559
12	Mg	$3s^2$	^1S	199.6146	199.6116	199.6107
13	Al	$3p^1$	^2P	241.8768	241.8733	241.8723
14	Si	$3p^2$	^3P	288.8545	288.8507	288.8495
15	P	$3p^3$	^4S	340.7193	340.7150	340.7137
16	S	$3p^4$	^3P	397.5063	397.5016	397.5002
17	Cl	$3p^5$	^2P	459.4826	459.4776	459.4760
18	Ar	$3p^6$	^1S	526.8175	526.8122	526.8105
19	K	$4s^1$	^2S	599.1649	599.1591	599.1571
20	Ca	$4s^2$	^1S	676.7582	676.7519	676.7497
21	Sc	$3d^14s^2$	^2D	759.7359	759.7277	759.7249
22	Ti	$3d^24s^2$	^3F	848.4066	848.3974	848.3942
23	V	$3d^34s^2$	^4F	942.8856	942.8760	942.8729
24	Cr	$3d^54s^1$	^7S	1043.3568	1043.3457	1043.3422
		$3d^44s^2$	^5D	1043.3121	1043.3024	1043.2993
25	Mn	$3d^54s^2$	^6S	1149.8698	1149.8600	1149.8569
26	Fe	$3d^64s^2$	^5D	1262.4500	1262.4380	1262.4344
		$3d^74s^1$	^5F	1262.3800	1262.3686	1262.3644
27	Co	$3d^74s^2$	^4F	1381.4186	1381.4056	1381.4018
28	Ni	$3d^84s^2$	^3F	1506.8732	1506.8598	1506.8560
29	Cu	$3d^{10}4s^1$	^2S	1638.9642	1638.9523	1638.9481
		$3d^94s^2$	^2D	1638.9509	1638.9374	1638.9338
30	Zn	$3d^{10}4s^2$	^1S	1777.8481	1777.8344	1777.8307
31	Ga	$4p^1$	^2P	1923.2612	1923.2487	1923.2454
32	Ge	$4p^2$	^3P	2075.3603	2075.3483	2075.3453
33	As	$4p^3$	^4S	2234.2399	2234.2281	2234.2251
34	Se	$4p^4$	^3P	2399.8691	2399.8573	2399.8543
35	Br	$4p^5$	^2P	2572.4418	2572.4300	2572.4269
36	Kr	$4p^6$	^1S	2752.0550	2752.0430	2752.0398
37	Rb	$5s^1$	^2S	2938.3576	2938.3455	2938.3421
38	Sr	$5s^2$	^1S	3131.5457	3131.5334	3131.5299
39	Y	$4d^15s^2$	^2D	3331.6846	3331.6710	3331.6670
40	Zr	$4d^35s^1$	^5F	3539.0117	3538.9970	3538.9925
		$4d^25s^2$	^3F	3538.9966	3538.9823	3538.9778
41	Nb	$4d^45s^1$	^6D	3753.6006	3753.5855	3753.5807
		$4d^35s^2$	^4F	3753.5550	3753.5403	3753.5355
42	Mo	$4d^55s^1$	^7S	3975.5530	3975.5371	3975.5320
43	Tc	$4d^55s^2$	^6S	4204.7949	4204.7793	4204.7741
		$4d^65s^1$	^6D	4204.7845	4204.7683	4204.7629
44	Ru	$4d^75s^1$	^5F	4441.5409	4441.5245	4441.5190
45	Rh	$4d^85s^1$	^4F	4685.8822	4685.8656	4685.8600

TABLE I (*Continued*).

Z	Atom	Configuration	Term	SUHF	OEP	KLI
46	Pd	$4d^{10}5s^0$	^1S	4937.9210	4937.9060	4937.9016
		$4d^95s^1$	^3D	4937.8936	4937.8766	4937.8710
		$4d^85s^2$	^3F	4937.7845	4937.7664	4937.7605
47	Ag	$4d^{10}5s^1$	^2S	5197.6989	5197.6815	5197.6758
48	Cd	$4d^{10}5s^2$	^1S	5465.1331	5465.1144	5465.1084
49	In	$5p^1$	^2P	5740.1694	5740.1514	5740.1455
50	Sn	$5p^2$	^3P	6022.9325	6022.9149	6022.9092
51	Sb	$5p^3$	^4S	6313.4870	6313.4697	6313.4639
52	Te	$5p^4$	^3P	6611.7856	6611.7683	6611.7625
53	I	$5p^5$	^2P	6917.9814	6917.9642	6917.9582
54	Xe	$5p^6$	^1S	7232.1384	7232.1210	7232.1150
55	Cs	$6s^1$	^2S	7553.9338	7553.9165	7553.9103
56	Ba	$6s^2$	^1S	7883.5438	7883.5266	7883.5201
79	Au	$5d^{10}6s^1$	^2S	17 865.4006	17 865.3703	17 865.3616
80	Hg	$5d^{10}6s^2$	^1S	18 408.9915	18 408.9605	18 408.9514

B. Highest occupied eigenvalues corresponding to each spin orientation

The KS energy eigenvalues have no physical interpretations except for the highest occupied one, which, according to Perdew *et al.* [4], exactly equals the negative of the removal energy of the electron system. In a spin-polarized exchange-only KS theory, i.e., the OEP formalism, it has been proved [24] that the $\varepsilon_{m\sigma}$ of each spin projection exactly equals the corresponding expectation value of the HF single-particle Hamiltonian, i.e., Koopmans's theorem applies for these states. The KLI construction, although merely an approximation to the KS theory, exactly satisfies this property as well [10–12]. In this work, since we are restricted to the exchange-only case, it is important to examine how accurate the KLI $\varepsilon_{m\sigma}$ are in approximating the two *exact* $\varepsilon_{m\sigma}$ values of HF and OEP.

In Table II, we present the negative values of $\varepsilon_{m\sigma}$. In this table, the atoms are grouped according to their outershell electron configuration. Both $\varepsilon_{m\uparrow}$ and $\varepsilon_{m\downarrow}$ are tabulated. In all cases, the state with up spin is always assumed to be filled first. For atoms with complete subshells, spins are indistinct, so only one ε_m is shown.

For OEP, instead of $\varepsilon_{m\sigma}$, we list the $\bar{\varepsilon}^{\mathrm{HF}}_{m\sigma}$ values. Although, as previously discussed, these two values should be the same in theory, this is not necessarily exactly the case in a numerical calculation. Our experience shows that without great caution, the two may be significantly different. Generally speaking, the $\bar{\varepsilon}^{\mathrm{HF}}_{m\sigma}$ will be a better and more reliable approximation to the theoretically exact $\varepsilon_{m\sigma}$ value than those directly calculated [12]. The latter depends very sensitively on the accurate solution of the OEP potential both in shape and magnitude. In applying the condition that $V_{x\sigma}\rightarrow -1/r$ as $r\rightarrow\infty$, one may introduce error if the cutoff point is applied before $V_{x\sigma}$ reaches the asymptotic region, i.e., the region in which the highest-energy occupied state dominates the density. The $\bar{\varepsilon}^{\mathrm{HF}}_{m\sigma}$, on the other hand, depends only on the wave function, thus is only indirectly affected by the change of the potential. In this work, nearly 80% of the reported calculations achieved agreement between the $\varepsilon_{m\sigma}$ and $\bar{\varepsilon}^{\mathrm{HF}}_{m\sigma}$ to within less than 0.1 mRy. Another 15% lies between 0.1 to a few millirydbergs. Larger errors, which run from 30 to 70 mRy, occur for the $4s\uparrow$ or $5s\uparrow$ state of a few transition elements: Cr(^7S), Y(^2D), Zr(^5F), Nb(^6D), and Mo(^7S). The reason for this may be attributed to the fact that in these atoms, the extended $(n-1)d$ state is competing with the ns state for the domination of the density in the outer region. In these cases, the $\varepsilon_{s\sigma}$ and $\varepsilon_{d\sigma}$ are very close to each other. Thus, it is difficult to determine which of the two states is actually the dominant one and where it becomes so. In fact, two different choices of mesh spacing for Sc(^2D) yield $\varepsilon_{m\sigma}$ values that are significantly different: 0.4068 and 0.4382 Ry, respectively. Nevertheless, for both mesh choices, all the other properties, the total energy and other expectation values like $\bar{\varepsilon}^{\mathrm{HF}}_{m\sigma}$ and $\langle r^n\rangle$ ($n=-1$, -2, 1, 2), are the same to all the digits reported. Other $\varepsilon_{m\sigma}$ values having larger errors may similarly be improved and become closer to $\bar{\varepsilon}^{\mathrm{HF}}_{m\sigma}$ if more care is taken. Nevertheless, we do not anticipate any significant changes for the $\bar{\varepsilon}^{\mathrm{HF}}_{m\sigma}$ values.

A glance at Table II immediately shows that the results of SUHF, OEP, and KLI are very close to each other. As is well known, the LSDX $\varepsilon_{m\sigma}$ are in error by about 40%, which is due primarily to the fact that its exchange potential approaches zero much too rapidly and therefore underestimates the magnitude of $\varepsilon_{m\sigma}$, so we do not list the LSDX $\varepsilon_{m\sigma}$ values and in the following we will in general not consider them further.

In the OEP calculations, larger differences of $\varepsilon_{m\sigma}$ from those of HF, the $\varepsilon^{\mathrm{HF}}_{m\sigma}$, come from some of the transition- and noble-metal elements, which can be as large as 8.1 mRy absolutely [for $3d\downarrow$ of Cu(^2S)] or 1.6% relatively [for $5s\uparrow$ of Zr(^5F)]. For all other atoms, the differences are never more than 3.4 mRy (for $2s\downarrow$ of O) or 0.6% ($4p\uparrow$ of Ga). In many cases, the two are different by merely a few tenths of a millirydberg.

TABLE II. Highest occupied energy eigenvalues, $(-\varepsilon_{m\sigma})$, of each spin projection in various exchange-only approximations. Atoms with complete subshells have the same $\varepsilon_{m\uparrow}$ and $\varepsilon_{m\downarrow}$, so only one value is listed. The state with up spin is always assumed to be filled first. For OEP, instead of $\varepsilon_{m\sigma}$, the corresponding expectation value of the HF single-particle Hamiltonian, $\bar{\varepsilon}^{\mathrm{HF}}_{m\sigma}$, is given. Theoretically [24], $\varepsilon_{m\sigma}=\bar{\varepsilon}^{\mathrm{HF}}_{m\sigma}$, but may not be exactly so numerically. The $\bar{\varepsilon}^{\mathrm{HF}}_{m\sigma}$ is in general a better estimate for the exact $\varepsilon_{m\sigma}$ (see Ref. [12] and this text). Occasionally in the OEP and KLI columns, values are marked by an asterisk, which represents the case that the order of the state yielding the highest-energy eigenvalue corresponding to a spin projection is changed as compared to the SUHF theory. The state directly below the ones with an asterisk has the highest $\varepsilon_{i\sigma},\varepsilon_{m'\sigma}$ in these calculations. For OEP and KLI, the value with an asterisk is the $\bar{\varepsilon}^{\mathrm{HF}}_{m\sigma}$; the value in parentheses is obtained by shifting all the directly calculated $\varepsilon_{i\sigma}$ such that $\varepsilon_{m\sigma}$ is aligned with $\bar{\varepsilon}^{\mathrm{HF}}_{m\sigma}$. Values are in rydbergs.

Z	Atom	Configuration	Term	State	SUHF	OEP	KLI
		Atoms with last filled subshell an s subshell					
4	Be	$2s^2$	^1S	$2s$	0.6185	0.6185	0.6177
12	Mg	$3s^2$	^1S	$3s$	0.5061	0.5060	0.5048
20	Ca	$4s^2$	^1S	$4s$	0.3911	0.3913	0.3901
38	Sr	$5s^2$	^1S	$5s$	0.3569	0.3573	0.3564
56	Ba	$6s^2$	^1S	$6s$	0.3151	0.3155	0.3148
30	Zn	$3d^{10}4s^2$	^1S	$4s$	0.5850	0.5855	0.5837
48	Cd	$4d^{10}5s^2$	^1S	$5s$	0.5297	0.5310	0.5301
80	Hg	$5d^{10}6s^2$	^1S	$6s$	0.5221	0.5240	0.5240
			Noble-gas atoms				
10	Ne	$2p^6$	^1S	$2p$	1.7008	1.7014	1.6988
18	Ar	$3p^6$	^1S	$3p$	1.1820	1.1816	1.1786
36	Kr	$4p^6$	^1S	$4p$	1.0484	1.0468	1.0440
54	Xe	$5p^6$	^1S	$5p$	0.9146	0.9129	0.9109
			Alkalis				
3	Li	$2s^1$	^2S	$2s\uparrow$	0.3927	0.3926	0.3924
				$1s\downarrow$	4.9374	4.9377	4.9343
11	Na	$3s^1$	^2S	$3s\uparrow$	0.3644	0.3642	0.3640
				$2p\downarrow$	3.0341	3.0354	3.0311
19	K	$4s^1$	^2S	$4s\uparrow$	0.2953	0.2954	0.2954
				$3p\downarrow$	1.9070	1.9069	1.9011
37	Rb	$5s^1$	^2S	$4s\uparrow$	0.2762	0.2766	0.2768
				$4p\downarrow$	1.6183	1.6171	1.6123
55	Cs	$6s^1$	^2S	$6s\uparrow$	0.2478	0.2483	0.2486
				$5p\downarrow$	1.3653	1.3638	1.3602
			Halogens				
9	F	$2p$	^2P	$2p\uparrow$	1.5396	1.5401	1.5387
				$2p\downarrow$	1.3475	1.3469	1.3449
17	Cl	$3p^5$	^2P	$3p\uparrow$	1.0584	1.0577	1.0550
				$3p\downarrow$	0.9467	0.9460	0.9436
35	Br	$4p^5$	^2P	$4p\uparrow$	0.9550	0.9533	0.9506
				$4p\downarrow$	0.8550	0.8532	0.8509
53	I	$5p^5$	^2P	$5p\uparrow$	0.8414	0.8396	0.8376
				$5p\downarrow$	0.7554	0.7537	0.7521
		Atoms with incomplete p subshell					
5	B	$2p^1$	^2P	$2p\uparrow$	0.6219	0.6194	0.6191
				$2s\downarrow$	0.8909	0.8909	0.8906
6	C	$2p^2$	^3P	$2p\uparrow$	0.8711	0.8705	0.8698
				$2s\downarrow$	1.1647	1.1645	1.1638
7	N	$2p^3$	^4S	$2p\uparrow$	1.1418	1.1423	1.1409
				$2s\downarrow$	1.4516	1.4515	1.4500
8	O	$2p^4$	^3P	$2p\uparrow$	1.3572	1.3579	1.3573
				$2p\downarrow$	1.0187	1.0153	1.0138
13	Al	$3p^1$	^2P	$3p\uparrow$	0.4200	0.4189	0.4171
				$3s\downarrow$	0.7264	0.7266	0.7255
14	Si	$3p^2$	^3P	$3p\uparrow$	0.5947	0.5933	0.5915
				$3s\downarrow$	0.9236	0.9237	0.9224

TABLE II. (*Continued*).

Z	Atom	Configuration	Term	State	SUHF	OEP	KLI
15	P	$3p^3$	^4S	$3p\uparrow$	0.7842	0.7831	0.7810
				$3s\downarrow$	1.1123	1.1124	1.1108
16	S	$3p^4$	^3P	$3p\uparrow$	0.9275	0.9267	0.9243
				$3p\downarrow$	0.7281	0.7273	0.7253
31	Ga	$4p^1$	^2P	$4p\uparrow$	0.4176	0.4150	0.4116
				$4s\downarrow$	0.7890	0.7899	0.7892
32	Ge	$4p^2$	^3P	$4p\uparrow$	0.5758	0.5734	0.5706
				$4s\downarrow$	0.9572	0.9577	0.9573
33	As	$4p^3$	^4S	$4p\uparrow$	0.7404	0.7382	0.7355
				$4s\downarrow$	1.1121	1.1123	1.1119
34	Se	$4p^4$	^3P	$4p\uparrow$	0.8543	0.8525	0.8498
				$4p\downarrow$	0.6708	0.6688	0.6669
49	In	$5p^1$	^2P	$5p\uparrow$	0.3954	0.3932	0.3904
				$5s\downarrow$	0.6901	0.6914	0.6914
50	Sn	$5p^2$	^3P	$5p\uparrow$	0.5315	0.5295	0.5272
				$5s\downarrow$	0.8202	0.8211	0.8215
51	Sb	$5p^3$	^4S	$5p\uparrow$	0.6715	0.6694	0.6673
				$5s\downarrow$	0.9378	0.9386	0.9392
52	Te	$5p^4$	^3P	$5p\uparrow$	0.7620	0.7602	0.7580
				$5p\downarrow$	0.6022	0.6004	0.5992
			First Transition Elements				
21	Sc	$3d^14s^2$	^2D	$4s\uparrow$	0.4331	0.4354	0.4381*
				$(3d\uparrow)$			(0.4182)
				$4s\downarrow$	0.4079	0.4066	0.4049
22	Ti	$3d^24s^2$	^3F	$4s\uparrow$	0.4647	0.4669	0.4709
				$4s\downarrow$	0.4203	0.4191	0.4161
23	V	$3d^34s^2$	^4F	$4s\uparrow$	0.4941	0.4963	0.5005
				$4s\downarrow$	0.4317	0.4307	0.4272
24	Cr	$3d^54s^1$	^7S	$4s\uparrow$	0.4441	0.4483	0.4551
				$3p\downarrow$	3.6797	3.6726	3.6972
		$3d^44s^2$	^5D	$4s\uparrow$	0.5220	0.5243	0.5282
				$4s\downarrow$	0.4424	0.4415	0.4378
25	Mn	$3d^54s^2$	^6S	$4s\uparrow$	0.5469	0.5492	0.5532
				$4s\downarrow$	0.4521	0.4512	0.4472
26	Fe	$3d^64s^2$	^5D	$4s\uparrow$	0.5543	0.5550	0.5558
				$4s\downarrow$	0.4843	0.4845	0.4835
		$3d^74s^1$	^5F	$4s\uparrow$	0.4579	0.4605	0.4667
				$(3d\uparrow)$			
				$3d\downarrow$	0.6239	0.6178	0.6388
27	Co	$3d^74s^2$	^4F	$4s\uparrow$	0.5617	0.5624	0.5614
				$4s\downarrow$	0.5111	0.5113	0.5108
28	Ni	$3d^84s^2$	^3F	$4s\uparrow$	0.5693	0.5699	0.5684
				$4s\downarrow$	0.5371	0.5374	0.5366
			Second Transition Elements				
39	Y	$4d^15s^2$	^2D	$5s\uparrow$	0.4103	0.4144*	0.4168*
				$(4d\uparrow)$		(0.3545)	(0.3380)
				$5s\downarrow$	0.3752	0.3740	0.3740
40	Zr	$4d^35s^1$	^5F	$5s\uparrow$	0.4125	0.4189*	0.4256*
				$(4d\uparrow)$		(0.3613)	(0.3512)
				$4p\downarrow$	2.6375	2.6350	2.6489
		$4d^25s^2$	^3F	$5s\uparrow$	0.4475	0.4517	0.4555
				$(4d\uparrow)$			
				$5s\downarrow$	0.3848	0.3836	0.3825
41	Nb	$4d^45s^1$	^6D	$5s\uparrow$	0.4321	0.4378	0.4446*
				$(4d\uparrow)$			(0.4316)
				$4p\downarrow$	2.9005	2.8980	2.9116
		$4d^35s^2$	^4F	$5s\uparrow$	0.4795	0.4835	0.4878
				$5s\downarrow$	0.3930	0.3920	0.3903

TABLE II. (*Continued*).

Z	Atom	Configuration	Term	State	SUHF	OEP	KLI
42	Mo	$4d^5 5s^1$	^7S	$5s\uparrow$	0.4461	0.4512	0.4582
				$4p\downarrow$	3.1459	3.1433	3.1570
43	Tc	$d^5 5s^2$	^6S	$5s\uparrow$	0.5318	0.5355	0.5403
				$5s\downarrow$	0.4061	0.4055	0.4031
		$4d^6 5s^1$	^6D	$5s\uparrow$	0.4457	0.4501	0.4563
				$4d\downarrow$	0.5176	0.5172	0.5274
44	Ru	$4d^7 5s^1$	^5F	$5s\uparrow$	0.4437	0.4474	0.4534
				$4d\downarrow$	0.6871	0.6843	0.6909
45	Rh	$4d^8 5s^1$	^4F	$5s\uparrow$	0.4427	0.4458	0.4513
				$4d\downarrow$	0.8140	0.8104	0.8151
46	Pd	$4d^{10} 5s^0$	^1S	$4d$	0.6720	0.6702	0.6725
		$4d^9 5s^1$	^3D	$5s\uparrow$	0.4423	0.4449	0.4500
				$4d\downarrow$	0.9308	0.9266	0.9302
		$4d^8 5s^2$	^3F	$5s\uparrow$	0.5290	0.5308	0.5306
				$5s\downarrow$	0.4873	0.4883	0.4877
			Noble-Metal	Atoms			
29	Cu	$3d^{10} 4s^1$	^2S	$4s\uparrow$	0.4793	0.4810	0.4880
				$(3d\uparrow)$			
				$3d\downarrow$	0.9866	0.9785	0.9968
		$3d^9 4s^2$	^2D	$4s\uparrow$	0.5771	0.5776	0.5760
				$4s\downarrow$	0.5623	0.5628	0.5614
47	Ag	$4d^{10} 5s^1$	^2S	$5s\uparrow$	0.4420	0.4443	0.4490
				$4d\downarrow$	1.0729	1.0684	1.0714
79	Au	$5d^{10} 6s^1$	^2S	$6s\uparrow$	0.4439	0.4469	0.4527
				$5d\downarrow$	1.0386	1.0329	1.0370

In the KLI approximation, similar to the OEP formalism, larger discrepancies mainly come from some of the transition- or noble-metal atoms. We have the largest absolute difference between the KLI $\varepsilon_{m\sigma}$ and $\varepsilon_{m\sigma}^{\rm HF}$ of 17.5 mRy for the $3p\downarrow$ state of Cr(^7S) and the largest relative disagreement of 3.2% for the $4s\uparrow$ state of Zr(^5F). The differences for other atoms are bounded by 6 mRy or 1.4% for the $4p\uparrow$ state of Ga, with many of them having errors of only a few tenths of a millirydberg. In general, the agreement between the KLI $\varepsilon_{m\sigma}$ and $\varepsilon_{m\sigma}^{\rm HF}$ are just slightly poorer than those of the OEP $\varepsilon_{m\sigma}$ and $\varepsilon_{m\sigma}^{\rm HF}$.

In comparing the KLI $\varepsilon_{m\sigma}$ with the OEP $\varepsilon_{m\sigma}$, again relative poorer agreement occurs for atoms in the transition or noble-metal group. We have a 24.6-mRy difference for the $3p\downarrow$ state of Cr(^7S) and a 1.9% error for the $3d\downarrow$ of Cu(^2S) between the KLI and OEP $\varepsilon_{m\sigma}$ values. The $\varepsilon_{m\sigma}$ for all other atoms are in closer agreement, being within 0.4% of the OEP results with an average difference of only about 0.2%.

We also make an observation on the peculiar behavior of the OEP and KLI calculations for a few transition- and noble-metal atoms. Occasionally, in Table II, a value is marked with an asterisk and below it another value is added in parentheses. These represent the cases where there is a reversal of the order of the state yielding the highest occupied energy eigenvalue for a given spin projection (in this work all occur in the up-spin direction) as compared to that of the SUHF. In the OEP calculation there are only two such cases, Y(^2D) and Zr(^5F), where unlike the SUHF, the eigenvalue of $4d\uparrow$ lies above that of $5s\uparrow$. In KLI, there are a couple of more cases. This may be understood as follows: Eigenvalues other than the highest occupied one have no physical interpretations in the KS formalism. Compared to the SUHF, all eigenvalues of the inner shells are raised. In all cases, where there is a reversal, the corresponding SUHF values for the two last subshells (states) are not very much separated. Thus, the raising of the eigenvalue for this inner subshell state may be larger than the difference of the two SUHF eigenvalues, resulting in the reversal of the order for the eigenvalues of the two states. In addition, notice that the reversal always happens to the ns and $(n-1)d$ state. Because of the high degeneracy of the d state, it is difficult to describe precisely the s-d interaction via a single potential. For KLI, where further approximation is made and the s-d interaction is still less well described, one finds more cases of reversal.

However, since in exchange-only calculations, only the expectation values of the single-particle HF Hamiltonian, $\bar{\varepsilon}_{i\sigma}^{\rm HF}$, have the physical interpretation of being the negative removal energy without relaxation [12] (the state with the highest $\bar{\varepsilon}_{i\sigma}^{\rm HF}$, $\varepsilon_{m\sigma}^{\rm HF}$ is still the same as those of the SUHF), and because the identity $\varepsilon_{i\sigma}=\bar{\varepsilon}_{i\sigma}^{\rm HF}$ holds only for the state having the highest $\varepsilon_{i\sigma},\varepsilon_{m'\sigma}$ (m' may or may not be the same as m), we thus conclude that for those atoms which have the reverse order ($m'\neq m$), the direct KS solutions for $\varepsilon_{m'\sigma}$ will merely give the second removal energy (without relaxation) and miss the first one, the $\bar{\varepsilon}_{m\sigma}^{\rm HF}$. In view of this, in Table II, we still list the $\bar{\varepsilon}_{m\sigma}^{\rm HF}$ values for the OEP calculations (with an asterisk); values in parentheses are obtained by shifting all the directly calculated $\varepsilon_{i\sigma}$ such that the $\varepsilon_{m\sigma}$ is aligned with $\bar{\varepsilon}_{m\sigma}^{\mathrm{HF}}$. Similar alignments have been made for the KLI results. In spite of the fact that there has been a reversal, if we reexamine the total energies in Table I and continue to study the results in the next section, we will see that it actually does not prevent us from obtaining accurate results by using the OEP or KLI.

We point out here that this peculiar behavior (of reversal) also occurs in the LSDX calculations and in fact there are more such cases. Actually, there is still another peculiar behavior which occurs only in the LSDX calculation that in a few cases, the order of the LSDX $\varepsilon_{m\uparrow}$ and $\varepsilon_{m\downarrow}$ is switched. Take Fe(^5F) for example: Whereas the SUHF, OEP, and KLI all predict that the highest spin up state $\varepsilon_{4s\uparrow}$ lies above the highest spin down state of $\varepsilon_{3d\downarrow}$, with a difference around 0.6 Ry, the LSDX yields a $\varepsilon_{3d\downarrow}$ which is 0.23 Ry above the $\varepsilon_{4s\uparrow}$. The correct description for these atoms by the KLI method is yet another evidence showing itself to be a much improved and accurate KS approximation as compared to the LSDX.

Finally, we study spin splitting of the highest occupied energy eigenvalues for atoms with $\varepsilon_{m\downarrow}$ and $\varepsilon_{m\uparrow}$ having the same spatial quantum numbers. The spin splitting, $\varepsilon_{m\downarrow}, -\varepsilon_{m\uparrow}$ is the difference between the highest occupied eigenvalues of minority (↓) and majority (↑) spin states. For SUHF, OEP, and KLI, it can be deduced from Table II. For convenience, we present them along with the LSDX result in Table III.

Clearly, for *p* states, the SUHF, OEP, and KLI yield spin splittings that are very close to each other. The differences between the OEP and SUHF results are less than 0.2 mRy (or less than 0.11%), except for atoms O and F which have a difference of 4.1 mRy (or about 1.2%) and 1.1 mRy (0.57%), respectively. The KLI results are never different from the OEP values by more than 1.0 mRy (or less than 0.6%). On the other hand, compared to the OEP, the LSDX values are significantly in error. The differences between the LSDX values and those of the OEP (or SUHF, or KLI) are more than 30 mRy and account for only 78% or less of the latter.

For *ns* states, where there is always an incomplete $(n-1)d$ subshell, the resemblances of the SUHF, OEP, and KLI values become less apparent. The differences are particularly larger for atoms with no $(n-1)d$ electrons in the minority spin projection (↓), where a typical difference of a few millirydbergs may occur which represents a few tens percent relatively and is yet another noticeable difference between the two *exact* exchange-only theories in treating electrons with the *s*-*d* interaction. For these atoms, the LSDX results may accidentally turn out to be closer to the SUHF values than those of the OEP as for atoms Y(^2D), Zr(^3F), and Nb(^4F) or closer to the OEP values than those of KLI as for a few more atoms. As the $(n-1)d\downarrow$ state is progressively filled, however, the SUHF, OEP, and KLI values once again become similar as is seen from the results for atoms Fe(^4F), Co(^4F), Ni(^4F), and Cu(^4F), and also Tc(^6S) and Pd(^3F) in Table III.

Spin splitting stems from the difference of the exchange

TABLE III. Spin splitting, $\varepsilon_{m\downarrow}-\varepsilon_{m\uparrow}$, of the highest occupied energy eigenvalues between the minority (↓) and majority (↑) spin states. In all cases, $\varepsilon_{m\downarrow}$ and $\varepsilon_{m\uparrow}$ have the same quantum numbers except for the opposite spin projections. Values are given in Rydbergs.

Z	Atom	Configuration	Term	SUHF	OEP	KLI	LSDX
			$\varepsilon_{np\downarrow}-\varepsilon_{np\uparrow}$				
8	O	$2p^4$	^3P	0.3385	0.3426	0.3435	0.2662
9	F	$2p^5$	^2P	0.1921	0.1932	0.1938	0.1390
16	S	$3p^4$	^3P	0.1994	0.1994	0.1990	0.1505
17	Cl	$3p^5$	^2P	0.1117	0.1117	0.1114	0.0758
34	Se	$4p^4$	^3P	0.1835	0.1837	0.1829	0.1303
35	Br	$4p^5$	^2P	0.1000	0.1001	0.0997	0.0637
52	Te	$5p^4$	^3P	0.1598	0.1598	0.1588	0.1095
53	I	$5p^5$	^2P	0.0860	0.0859	0.0855	0.0527
			$\varepsilon_{ns\downarrow}-\varepsilon_{ns\uparrow}$				
21	Sc	$3d^14s^2$	^2D	0.0252	0.0288	0.0332	0.0316
22	Ti	$3d^24s^2$	^3F	0.0444	0.0478	0.0548	0.0540
23	V	$3d^34s^2$	^4F	0.0624	0.0656	0.0733	0.0722
24	Cr	$3d^44s^2$	^5D	0.0796	0.0828	0.0904	0.0882
25	Mn	$3d^54s^2$	^6S	0.0948	0.0980	0.1060	0.1026
26	Fe	$3d^64s^2$	^5D	0.0700	0.0705	0.0723	0.0719
27	Co	$3d^74s^2$	^4F	0.0506	0.0511	0.0506	0.0489
28	Ni	$3d^84s^2$	^3F	0.0322	0.0325	0.0318	0.0300
29	Cu	$3d^94s^2$	^2D	0.0148	0.0148	0.0146	0.0141
39	Y	$4d^15s^2$	^2D	0.0351	0.0404	0.0428	0.0383
40	Zr	$4d^25s^2$	^3F	0.0627	0.0681	0.0730	0.0652
41	Nb	$4d^35s^2$	^4F	0.0865	0.0915	0.0975	0.0860
43	Tc	$4d^55s^2$	^6S	0.1257	0.1300	0.1372	0.1172
46	Pd	$4d^85s^2$	^3F	0.0417	0.0425	0.0429	0.0341

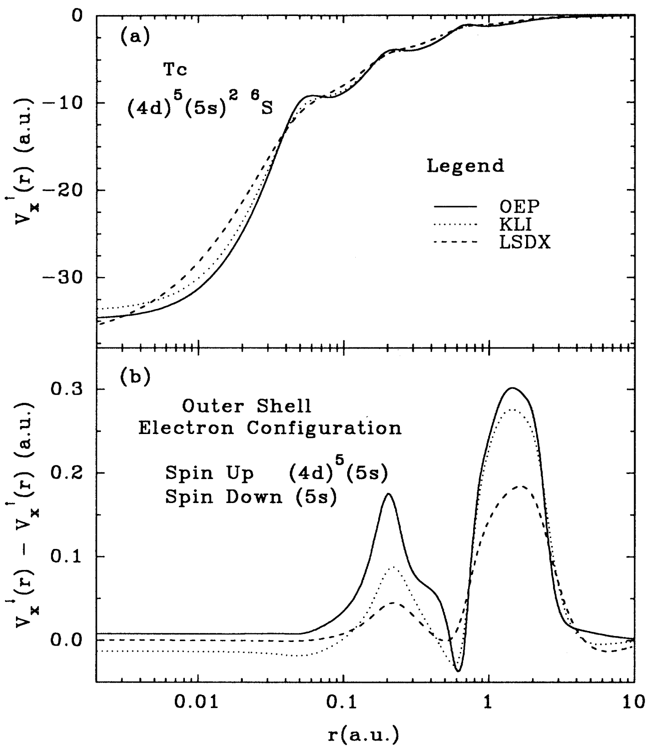

FIG. 2. (a) Exchange potentials for the majority spin projection (↑) of the atom Tc(^6S) from the OEP, KLI, and LSDX calculations. (b) Difference of the exchange potentials between the minority (↓) and majority (↑) spin projections for each method.

potentials of the minority and majority spin projections. In Fig. 2(a), we display the exchange potential of the majority spin projection (↑) for atom Tc(^6S), which has five electrons in the $4d\uparrow$ subshell and an empty $4d\downarrow$ subshell, the highest occupied states in both spin projections being the $5s$ state. The KLI potential is manifestly closer to the OEP than is the LSDX, which is a typical result for other atoms as well. In Fig. 2(b), the differences of the exchange potentials, $V_x^{\downarrow}(r)-V_x^{\uparrow}(r)$, are shown. The KLI difference is apparently more similar to the OEP curve than is the LSDX both in shape and magnitude, which is in agreement with the closer spin splitting of the KLI calculation than the LSDX as compared to the OEP values in Table III. The ΔV_x of the OEP and KLI are even more like each other for those atoms with np being the highest occupied state in both spin projections or with ns being the highest occupied state in both spin projections under the condition that $(n-1)d\downarrow$ subshell is partly filled and are less so for those transition elements with ns being the highest occupied state and having an empty $(n-1)d\downarrow$ subshell.

C. Expectation values

Table IV displays the results of $\langle r^2\rangle$, $\langle r^{-1}\rangle$, $\langle\delta(\mathbf{r})\rangle$, and the spin density at the origin, $m(0)=n_{\uparrow}(0)-n_{\downarrow}(0)$, from the SUHF, OEP, KLI, and LSDX calculations. The expectation values are important quantities in assessing the accuracy of the electron density [and the spin density in the case of $m(0)$] as obtained from an approximate KS solution: how close it is in comparison with the results of the SUHF and the OEP. Some of them directly relate to the physically observable and measurable properties such as the diamagnetic susceptibility ($\langle r^2\rangle$) and the Fermi contact term of the hyperfine structure [$m(0)$].

The expectation values depend only indirectly on the exchange potential. A glance at Table IV shows that, unlike the $\varepsilon_{m\sigma}$ values and except for data in the last column for $m(0)$, which is obtained from the difference of two large numbers, all calculations including those from LSDX yield similar results. In the following, we will conduct a detailed analysis.

1. $\langle r^2\rangle$ value

The value of $\langle r^2\rangle$ is heavily weighted by electrons in the outer subshells of the atom and provides a test of how well the electron density is approximated in the low-density region far from the nucleus which is of significance in chemical bonding.

From Table IV, it is seen that the OEP $\langle r^2\rangle$ results are very close to those of the SUHF. The largest discrepancy is only 1% for Cr(^7S). The majority are within a few tenths of a percent of each other. For most atoms, the KLI values are accurate to within a few tenths of a percent of the SUHF and OEP results. Less accurate are those atoms with s and d electrons in the last two shells. For these elements, an error up to 2% may occur. In nearly all cases, the KLI results are an order of magnitude more accurate than those of the LSDX.

2. $\langle r^{-1}\rangle$ value

The fact that $\sum_i 1/r_i$ appears in the Hamiltonian and the calculated expectation value of the energy are all very close to each other when SUHF, OEP, KLI, or LSDX is employed, suggests that the values of $\langle r^{-1}\rangle$ should similarly be close to each other. This is precisely what we find. In this case, the OEP results never deviate from the SUHF values by more than 52 ppm (for Li). In the worst case, the KLI has an error of only 0.08% (for Be) in comparison with either SUHF or OEP. The LSDX, generally many times less accurate, can result in a 1.7% error (for Li) in both comparisons. The fact that the Hartree potential at the origin (nucleus) is $Z\langle 1/r\rangle$ together with the observation that the SUHF, OEP, and KLI results for $\langle 1/r\rangle$ are nearly identical demonstrates that all three methods give nearly the same Hartree potential deep in the interior of the atom, with the LSDX generally yielding a Hartree potential that is too small.

Comparisons for other moments like $\langle r\rangle$ and $\langle r^{-2}\rangle$ (which are not displayed here) show similar patterns: the OEP and SUHF results are nearly identical, and the KLI results are in general a better approximation to the SUHF or OEP than those of LSDX.

TABLE IV. Expectation values of the single-particle operators, r^2, r^{-1}, $\delta(\mathbf{r})$, and $m(0)$, for atoms ($Z=3$–56, 79, 80) as obtained from various exchange-only approximations. Calculations are performed for the ground-state configuration and in a few cases for terms in the low-lying excited-energy-state configuration. Spin-unrestricted technique is employed in all cases where there are incomplete subshells. All values quoted are in atomic units.

Z	Atom	Method	$\langle r^2\rangle$	$\langle r^{-1}\rangle$	$\langle\delta(\mathbf{r})\rangle$	$m(0)$
3	Li(^2S)	SUHF	6.2080	1.9052	13.8148	0.2247
		OEP	6.2145	1.9051	13.8148	0.2249
		KLI	6.1974	1.9060	13.8254	0.2386
		LSDX	6.4685	1.8731	13.4736	0.2016
4	Be(^1S)	SUHF	4.3297	2.1022	35.3877	
		OEP	4.3316	2.1022	35.3877	
		KLI	4.3255	2.1039	35.4426	
		LSDX	4.4809	2.0766	34.7001	
5	B(^2P)	SUHF	3.1674	2.2760	71.9141	0.0171
		OEP	3.1690	2.2759	71.9161	0.0190
		KLI	3.1724	2.2770	71.9605	−0.0533
		LSDX	3.3918	2.2534	70.7746	−0.0214
6	C(^3P)	SUHF	2.2966	2.4484	127.420	0.0772
		OEP	2.2967	2.4484	127.421	0.0780
		KLI	2.2969	2.4488	127.382	−0.1556
		LSDX	2.4543	2.4284	125.687	−0.0345
7	N(^4S)	SUHF	1.7252	2.6196	205.866	0.1875
		OEP	1.7253	2.6196	205.869	0.1897
		KLI	1.7240	2.6194	205.636	−0.3338
		LSDX	1.8461	2.6011	203.403	−0.0519
8	O(^3P)	SUHF	1.4029	2.7823	311.611	0.1954
		OEP	1.4032	2.7823	311.618	0.1942
		KLI	1.4039	2.7817	311.102	−0.3159
		LSDX	1.5108	2.7646	308.248	−0.0325
9	F(^2P)	SUHF	1.1386	2.9465	448.309	0.1333
		OEP	1.1386	2.9465	448.313	0.1357
		KLI	1.1385	2.9455	447.349	−0.2142
		LSDX	1.2211	2.9298	443.867	−0.0234
10	Ne(^1S)	SUHF	0.9372	3.1113	619.922	
		OEP	0.9372	3.1113	619.930	
		KLI	0.9367	3.1100	618.310	
		LSDX	1.0036	3.0952	614.230	
11	Na(^2S)	SUHF	2.4673	3.2210	833.759	0.6474
		OEP	2.4708	3.2209	833.768	0.6449
		KLI	2.4574	3.2197	831.656	0.7237
		LSDX	2.4506	3.2074	826.626	0.7331
12	Mg(^1S)	SUHF	2.4676	3.3267	1093.72	
		OEP	2.4693	3.3267	1093.73	
		KLI	2.4610	3.3258	1091.15	
		LSDX	2.4575	3.3147	1085.12	
13	Al(^2P)	SUHF	2.5756	3.4231	1402.85	−0.1091
		OEP	2.5772	3.4231	1402.87	−0.1085
		KLI	2.5798	3.4225	1399.71	−0.1260
		LSDX	2.6668	3.4118	1392.60	−0.1427
14	Si(^3P)	SUHF	2.3037	3.5174	1765.61	−0.1547
		OEP	2.3042	3.5174	1765.62	−0.1610
		KLI	2.3068	3.5172	1761.85	−0.1841
		LSDX	2.3788	3.5069	1753.57	−0.2221
15	P(^4S)	SUHF	2.0173	3.6099	2186.30	−0.1394
		OEP	2.0174	3.6099	2186.30	−0.1576
		KLI	2.0188	3.6098	2181.85	−0.2128
		LSDX	2.0856	3.5998	2172.32	−0.2811
16	S(^3P)	SUHF	1.8267	3.6988	2669.45	−0.0088
		OEP	1.8269	3.6988	2669.46	−0.0265
		KLI	1.8281	3.6988	2664.16	−0.0600
		LSDX	1.8847	3.6892	2653.24	−0.1142
17	Cl(^2P)	SUHF	1.6264	3.7867	3219.18	0.0338
		OEP	1.6265	3.7867	3219.19	0.0238
		KLI	1.6273	3.7868	3212.99	−0.0103
		LSDX	1.6744	3.7776	3200.61	−0.0436
18	Ar(^1S)	SUHF	1.4464	3.8736	3839.78	
		OEP	1.4465	3.8736	3839.78	
		KLI	1.4467	3.8738	3832.60	
		LSDX	1.4889	3.8648	3818.69	
19	K(^2S)	SUHF	2.6936	3.9417	4538.66	0.8534
		OEP	2.6939	3.9417	4538.67	0.8598
		KLI	2.6785	3.9421	4530.49	0.9428
		LSDX	2.6087	3.9340	4514.86	0.9977
20	Ca(^1S)	SUHF	2.8283	4.0080	5319.61	
		OEP	2.8282	4.0080	5319.64	
		KLI	2.8174	4.0086	5310.47	
		LSDX	2.7503	4.0010	5293.06	
21	Sc(^2D)	SUHF	2.5334	4.0814	6182.31	−0.0239
		OEP	2.5258	4.0815	6182.32	−0.0314
		KLI	2.5075	4.0817	6172.14	0.0181
		LSDX	2.4788	4.0741	6153.05	0.0765
22	Ti(^3F)	SUHF	2.2838	4.1554	7133.25	−0.0673
		OEP	2.2792	4.1555	7133.24	−0.0891
		KLI	2.2581	4.1556	7121.87	−0.0973
		LSDX	2.2367	4.1480	7101.13	0.1466
23	V(^4F)	SUHF	2.0721	4.2293	8176.98	−0.1163
		OEP	2.0693	4.2293	8176.98	−0.1440
		KLI	2.0502	4.2292	8164.20	−0.3487
		LSDX	2.0317	4.2218	8141.78	0.2057
24	Cr(^7S)	SUHF	1.5691	4.3109	9313.73	1.0236
		OEP	1.5529	4.3110	9313.71	0.9603
		KLI	1.5226	4.3103	9299.32	0.7095
		LSDX	1.6059	4.3018	9275.23	2.1382
	(^5D)	SUHF	1.8902	4.3028	9313.88	−0.1709
		OEP	1.8883	4.3029	9313.88	−0.2010
		KLI	1.8720	4.3026	9303.54	−0.7085
		LSDX	1.8561	4.2954	9279.41	0.2539
25	Mn(^6S)	SUHF	1.7325	4.3764	10 560.1	−0.2381
		OEP	1.7313	4.3764	10 560.1	−0.2751
		KLI	1.7167	4.3759	10 544.2	−1.1141
		LSDX	1.7041	4.3688	10 518.4	0.2913
26	Fe(^5D)	SUHF	1.5869	4.4482	11 908.8	−0.2065
		OEP	1.5832	4.4483	11 908.7	−0.2204
		KLI	1.5595	4.4476	11 891.2	−1.2243
		LSDX	1.5543	4.4408	11 863.5	0.1920
	(^5F)	SUHF	1.3648	4.4554	11 903.6	1.9331
		OEP	1.3569	4.4555	11 903.6	1.8416
		KLI	1.3237	4.4547	11 885.4	2.1097
		LSDX	1.3972	4.4465	11 858.1	3.2138

TABLE IV. (*Continued*).

Z	Atom	Method	$\langle r^2\rangle$	$\langle r^{-1}\rangle$	$\langle\delta(\mathbf{r})\rangle$	$m(0)$	Z	Atom	Method	$\langle r^2\rangle$	$\langle r^{-1}\rangle$	$\langle\delta(\mathbf{r})\rangle$	$m(0)$
27	Co(^4F)	SUHF	1.4608	4.5203	13 367.4	−0.1629	39	Y(^2D)	SUHF	1.8841	5.2212	41 189.3	−0.0072
		OEP	1.4584	4.5204	13 367.3	−0.1608			OEP	1.8765	5.2213	41 189.4	0.0162
		KLI	1.4336	4.5195	13 348.0	−1.1442			KLI	1.8699	5.2207	41 138.9	0.3151
		LSDX	1.4277	4.5128	13 318.6	0.1187			LSDX	1.8404	5.2167	41 080.5	0.0979
28	Ni(^3F)	SUHF	1.3504	4.5921	14 940.6	−0.1156	40	Zr(^5F)	SUHF	1.5449	5.2724	44 499.4	2.1851
		OEP	1.3485	4.5922	14 940.5	−0.1146			OEP	1.5318	5.2725	44 499.5	2.2353
		KLI	1.3254	4.5912	14 919.2	−0.8764			KLI	1.5301	5.2717	44 445.8	3.0056
		LSDX	1.3187	4.5846	14 888.0	0.0637			LSDX	1.5828	5.2673	44 384.4	3.4004
29	Cu(^2S)	SUHF	1.1074	4.6716	16 625.3	3.3703		(^3F)	SUHF	1.7671	5.2698	44 504.3	−0.0788
		OEP	1.1020	4.6717	16 625.2	3.2417			OEP	1.7619	5.2698	44 504.5	−0.0678
		KLI	1.0741	4.6705	16 600.7	4.6454			KLI	1.7519	5.2692	44 450.9	0.4303
		LSDX	1.1148	4.6627	165 68.2	4.6909			LSDX	1.7297	5.2652	44 389.7	0.2138
	(^2D)	SUHF	1.2527	4.6638	16 632.6	−0.0633	41	Nb(^6D)	SUHF	1.4374	5.3212	47 987.2	2.0167
		OEP	1.2512	4.6639	16 632.5	−0.0657			OEP	1.4285	5.3212	47 987.4	2.0562
		KLI	1.2302	4.6627	16 609.0	−0.4650			KLI	1.4210	5.3205	47 930.5	2.9229
		LSDX	1.2234	4.6565	16 576.1	0.0246			LSDX	1.4643	5.3161	47 866.2	3.5486
30	Zn(^1S)	SUHF	1.1660	4.7355	18 447.7			(^4F)	SUHF	1.6629	5.3181	47 992.7	−0.1876
		OEP	1.1648	4.7356	18 447.6				OEP	1.6597	5.3182	47 992.7	−0.1759
		KLI	1.1453	4.7343	18 421.7				KLI	1.6498	5.3176	47 936.1	0.3896
		LSDX	1.1392	4.7280	18 387.2				LSDX	1.6294	5.3136	47 872.1	0.3197
31	Ga(^2P)	SUHF	1.3218	4.7952	20 397.2	−0.3464	42	Mo(^7S)	SUHF	1.3420	5.3697	51 652.8	1.7400
		OEP	1.3223	4.7952	20 397.2	−0.3454			OEP	1.3355	5.3698	51 653.0	1.7655
		KLI	1.3188	4.7940	20 368.8	−0.3750			KLI	1.3245	5.3691	51 593.0	2.7824
		LSDX	1.3448	4.7883	20 331.9	−0.4802			LSDX	1.3647	5.3646	51 525.8	3.6485
32	Ge(^3P)	SUHF	1.2999	4.8540	22 480.1	−0.5293	43	Tc(^6S)	SUHF	1.4832	5.4142	55 507.4	−0.5069
		OEP	1.2997	4.8540	22 480.2	−0.5568			OEP	1.4818	5.4143	55 507.6	−0.4984
		KLI	1.2990	4.8528	22 449.3	−0.5648			KLI	1.4737	5.4137	55 444.3	0.1927
		LSDX	1.3264	4.8476	22 410.0	−0.7706			LSDX	1.4572	5.4097	55 374.5	0.5069
33	As(^4S)	SUHF	1.2436	4.9119	24 701.0	−0.5970		(^6D)	SUHF	1.2880	5.4174	55 500.6	2.4598
		OEP	1.2432	4.9119	24 701.0	−0.6695			OEP	1.2828	5.4174	55 500.8	2.4745
		KLI	1.2433	4.9108	24 667.6	−0.6495			KLI	1.2680	5.4168	55 437.2	3.7417
		LSDX	1.2736	4.9058	24 625.9	−0.9975			LSDX	1.3020	5.4124	55 367.1	4.4771
34	Se(^3P)	SUHF	1.2130	4.9682	27 064.4	−0.2378	44	Ru(^5F)	SUHF	1.2294	5.4650	59 535.0	3.1697
		OEP	1.2130	4.9683	27 064.4	−0.3092			OEP	1.2252	5.4650	59 535.2	3.1660
		KLI	1.2135	4.9672	27 028.3	−0.2421			KLI	1.2097	5.4644	59 468.2	4.5338
		LSDX	1.2377	4.9625	26 983.9	−0.4688			LSDX	1.2358	5.4601	59 395.3	5.1685
35	Br(^2P)	SUHF	1.1582	5.0240	29 574.6	−0.0527	45	Rh(^4F)	SUHF	1.1749	5.5123	63 760.7	3.9067
		OEP	1.1581	5.0240	29 574.6	−0.0961			OEP	1.1715	5.5124	63 760.9	3.8898
		KLI	1.1588	5.0230	29 535.6	−0.0572			KLI	1.1558	5.5117	63 690.3	5.2661
		LSDX	1.1803	5.0185	29 488.6	−0.1924			LSDX	1.1745	5.5075	63 614.5	5.7794
36	Kr(^1S)	SUHF	1.0981	5.0792	32 235.9		46	Pd(^1S)	SUHF	0.9265	5.5629	68 175.5	
		OEP	1.0980	5.0792	32 235.9				OEP	0.9268	5.5629	68 175.6	
		KLI	1.0985	5.0783	32 194.1				KLI	0.9292	5.5623	68 100.3	
		LSDX	1.1196	5.0738	32 144.3				LSDX	0.9987	5.5573	68 021.8	
37	Rb(^2S)	SUHF	1.8422	5.1264	35 057.6	1.5642		(^3D)	SUHF	1.1237	5.5595	68 182.1	4.6668
		OEP	1.8409	5.1264	35 057.7	1.5920			OEP	1.1210	5.5595	68 182.3	4.6438
		KLI	1.8298	5.1257	35 012.9	1.6816			KLI	1.1055	5.5588	68 108.1	5.9657
		LSDX	1.7712	5.1216	34 960.3	1.8534			LSDX	1.1183	5.5547	68 029.2	6.3365
38	Sr(^1S)	SUHF	2.0016	5.1729	38 042.8			(^3F)	SUHF	1.2519	5.5557	68 192.1	−0.2806
		OEP	2.0006	5.1729	38 043.0				OEP	1.2499	5.5557	68 192.3	−0.2703
		KLI	1.9923	5.1723	37 995.1				KLI	1.2348	5.5551	68 119.0	−0.1326
		LSDX	1.9294	5.1685	37 939.7				LSDX	1.2227	5.5514	68 039.8	0.1698

TABLE IV. (*Continued*).

Z	Atom	Method	$\langle r^2 \rangle$	$\langle r^{-1} \rangle$	$\langle \delta(\mathbf{r}) \rangle$	$m(0)$	Z	Atom	Method	$\langle r^2 \rangle$	$\langle r^{-1} \rangle$	$\langle \delta(\mathbf{r}) \rangle$	$m(0)$
47	Ag(^2S)	SUHF	1.0750	5.6064	72 803.5	5.4310	53	I(^2P)	SUHF	1.1977	5.8481	105 056.3	−0.0978
		OEP	1.0728	5.6065	72 803.6	5.4110			OEP	1.1973	5.8481	105 056.5	−0.1738
		KLI	1.0577	5.6058	72 725.8	6.6409			KLI	1.1980	5.8477	104 954.2	−0.0916
		LSDX	1.0666	5.6016	72 644.0	6.8568			LSDX	1.2081	5.8447	104 849.3	−0.3060
48	Cd(^1S)	SUHF	1.1325	5.6490	77 641.6		54	Xe(^1S)	SUHF	1.1602	5.8866	111 219.4	
		OEP	1.1312	5.6491	77 641.7				OEP	1.1600	5.8866	111 219.6	
		KLI	1.1180	5.6484	77 561.0				KLI	1.1607	5.8863	111 112.7	
		LSDX	1.1065	5.6448	77 475.6				LSDX	1.1716	5.8833	111 003.7	
49	In(^2P)	SUHF	1.2549	5.6898	82 686.2	−0.4822	55	Cs(^2S)	SUHF	1.7776	5.9208	117 625.5	2.0146
		OEP	1.2544	5.6898	82 686.4	−0.4913			OEP	1.7757	5.9208	117 625.7	2.0665
		KLI	1.2512	5.6892	82 601.5	−0.5116			KLI	1.7662	5.9206	117 514.0	2.1286
		LSDX	1.2587	5.6858	82 512.4	−0.7117			LSDX	1.7017	5.9178	117 400.9	2.4047
50	Sn(^3P)	SUHF	1.2602	5.7301	87 945.3	−0.7338	56	Ba(^1S)	SUHF	1.9399	5.9547	124 276.9	
		OEP	1.2594	5.7302	87 945.5	−0.7939			OEP	1.9384	5.9547	124 277.2	
		KLI	1.2586	5.7296	87 856.4	−0.7748			KLI	1.9309	5.9546	124 160.6	
		LSDX	1.2702	5.7263	87 763.7	−1.1464			LSDX	1.8597	5.9519	124 043.5	
51	Sb(^4S)	SUHF	1.2356	5.7701	93 423.6	−0.8385	79	Au(^2S)	SUHF	0.8132	6.8207	353 747.4	9.8772
		OEP	1.2349	5.7701	93 423.8	−0.9727			OEP	0.8117	6.8207	353 747.9	9.9044
		KLI	1.2350	5.7696	93 330.5	−0.8931			KLI	0.8028	6.8193	353 489.4	11.7373
		LSDX	1.2511	5.7664	93 234.0	−1.4922			LSDX	0.8101	6.8173	353 279.6	12.0332
52	Te(^3P)	SUHF	1.2275	5.8093	99 125.9	−0.3568	80	Hg(^1S)	SUHF	0.8578	6.8516	367 542.1	
		OEP	1.2272	5.8093	99 126.1	−0.4855			OEP	0.8567	6.8517	367 542.8	
		KLI	1.2277	5.8088	99 028.2	−0.3494			KLI	0.8477	6.8503	367 277.8	
		LSDX	1.2387	5.8058	98 927.4	−0.7285			LSDX	0.8417	6.8486	367 062.5	

3. $\langle \delta(\mathbf{r}) \rangle$ values

As seen from the table, apart from a few exceptions, the OEP and SUHF $\langle \delta(\mathbf{r}) \rangle$ are identical to each other to all but the last quoted digit. The largest discrepancy is merely 28 ppm. The KLI results generally agree with those of the SUHF or OEP to three digits. The errors are between 0.06% to 0.3%. It is observed that all KLI $\langle \delta(\mathbf{r}) \rangle$ values except for the first three, Li, Be, and B, lie below either the SUHF or OEP and all the LSDX values lie still lower, typically being about twice as far from the SUHF or OEP results than those given by the KLI.

4. $m(0)$: Spin density at the nucleus

The spin density is obtained by taking the difference of the densities corresponding to each spin projection. Of particular interest is the spin density value at the nucleus, $m(0)$. Numerically, this value is difficult to calculate accurately, since it involves the subtraction of two very large numbers. In a SUHF calculation, Bagus, Liu, and Schaefer [30] have pointed out that without taking great care, one may get entirely erroneous results. Wherever available, our code yields SUHF values that deviate from theirs by at most one part in the last digit. In fact, in our SUHF calculations, the Virial relationship corresponding to $E=-T$, where E and T denote total energy and total kinetic energy, respectively, is satisfied to at least eight digits.

In the last column of Table IV, we list the $m(0)$ values as obtained from each calculation. Since only the s orbital density contributes to $m(0)$, we expect that $m(0)$ values for atoms with an unpaired s state should be larger than those atoms with only unpaired p or d states. The nonzero $m(0)$ from the latter comes entirely from the polarization of the paired s states due to the polarized p or d states. From the table, we see that in general this is indeed the case.

First, we compare the OEP results with those of the SUHF. From the table, we can see that for most atoms, the OEP values form a good approximation to the SUHF. In particular, for those atoms with an unpaired s state like the alkali metals and some in the transition series and noble-metal group, the two are different by at most 6.2% [Cr(^7S)]. Significant differences exist for atoms S(200%) and Y(329%), both of which, however, have very small values of $m(0)$.

For alkali metals, the KLI results provide a reasonable and always a better (over that of LSDX) estimate to $m(0)$ for both the SUHF and OEP. The largest error is around 10% (for K). For atoms in the transition- and noble-metal groups with an unpaired s state, the KLI and LSDX results generally overestimate the $m(0)$ values. The overestimate of the KLI ranges from about 10% [Fe(^5F)] to nearly 60% [Mo(^7S)] and that of LSDX is always larger. The only exception is for Cr(^7S), in which case the KLI $m(0)$ underestimates the HF or OEP result by about 30%, the corresponding LSDX values overestimating the $m(0)$ by more than 100%. For other atoms, although generally still an improvement over the LSDX, overall, the results cannot be regarded as reliable. Some of them even yield $m(0)$ that has an incorrect sign. In the worst case, it produces an error that is over 4000% (for Y), even though the separate spin densities $n_\uparrow(0)$ and $n_\downarrow(0)$ are different from the SUHF or OEP results by only approximately one part in a thousand.

The remarkably good agreement of the OEP $m(0)$ value with that of the SUHF is most remarkable, especially when one examines Table V, in which for selected atoms we list the spin-density contributions from each s subshell. It is seen that although the separate contributions from the OEP calculations are significantly different from those of the corresponding SUHF, some of them even having opposite signs, the net sum always tends to yield an $m(0)$ that accurately approximates the SUHF. This desirable cancellation process is typical for most other atoms as well; thus, as a whole, the OEP and SUHF values for $m(0)$ are very close. However, in KLI and LSDX calculations, the cancellation process ceases to be as perfect. As a result, the KLI and LSDX spin densities at the nucleus are in general not a very accurate approximation.

In fact, the close resemblance between the OEP and SUHF results for $m(0)$ continues to be true even for spin density $m(r)$ away from the nucleus. In Fig. 3, we display the $m(r)$ values of the SUHF, OEP, KLI, and LSDX calculations for the atom Tc(^6S) which has a filled $4d\uparrow$ subshell and an empty $4d\downarrow$ subshell. Both $5s\uparrow$ and $5s\downarrow$ states are occupied, so there is no unpaired s state. The spin polarization is mainly due to the unpaired five electrons in the $4d\uparrow$ state as is evidenced from the peaks in the $m(r)$ curve which coincide with the maxima of the $4d\uparrow$ state. Clearly, in all regions, including that near the nucleus, the OEP and SUHF curves are nearly indistinguishable, which is a typical result of the OEP calculations for most of the other atoms as well. On the other hand, the $m(r)$ of KLI and LSDX, although being a reasonable approximation to the OEP $m(r)$ in regions where the $4d\uparrow$ state density is dominant, fails to correctly mimic the $m(r)$ values in other regions, especially near the nucleus. This is also a quite typical result of the KLI

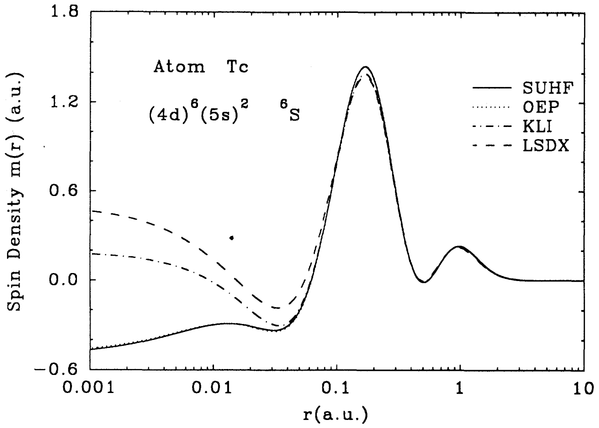

FIG. 3. Comparison of the spin density, $m(r)$ (in a.u.), for the atom Tc(^6S) vs r, the distance from the nucleus (in a.u., logarithmic scale), as obtained from each method.

TABLE V. Comparison of the contributions to the spin density at the nucleus $m(0)$ from each s orbital density for selected atoms in various exchange-only approximations (in a.u.).

Z	Atom		Configuration	$m_i(0)$	SUHF	OEP	KLI	LSDX
7	N(^4S)	↑	$1s2s2p^3$	1s	−0.7432	−0.5813	−1.0386	−0.6668
				2s	0.9307	0.7710	0.7048	0.6149
		↓	$1s2s$	net	0.1875	0.1897	−0.3338	−0.0519
19	K(^2S)	↑	$1s2s2p^33s3p^34s$	1s	0.0342	0.0250	0.0373	0.0139
				2s	0.0409	0.0023	0.0117	−0.0014
		↓	$1s2s2p^33s3p^3$	3s	0.0875	0.0027	−0.0012	−0.0475
				4s	0.6908	0.8298	0.8950	1.0327
				net	0.8534	0.8598	0.9428	0.9977
43	Tc(^6S)	↑	$1s2s2p^33s3p^33d^5$	1s	−0.0226	−0.1675	−0.0276	−0.0420
			$4s4p^34d^55s$	2s	−1.0345	−1.6023	−1.1135	−0.4819
				3s	0.3470	0.8773	0.4219	−0.0945
		↓	$1s2s2p^33s3p^33d^5$	4s	−2.5112	−2.8751	−2.5937	−1.5765
			$4s4p^35s$	5s	2.7144	3.2692	3.5056	2.7018
				net	−0.5069	−0.4984	0.1927	0.5069
79	Au(^2S)	↑	$1s2s2p^33s3p^33d^5$	1s	0.0832	−0.4722	0.1038	0.0303
			$4s4p^34d^54f^7$	2s	0.0907	−0.0912	0.0542	0.0128
			$5s5p^35d^56s$	3s	0.1333	−0.0590	0.0390	0.0088
				4s	0.1715	−0.0096	−0.0120	−0.0111
		↓	$1s2s2p^33s3p^33d^5$	5s	0.5685	−0.2203	−0.0861	−0.0570
			$4s4p^34d^54f^7$	6s	8.8300	10.7567	11.6384	12.0494
			$5s5p^35d^5$	net	9.8772	9.9044	11.7373	12.0332

and LSDX calculations showing that these approximations will in general only yield reasonable, but not as accurate as the OEP to SUHF, results for spin densities in the region where the unpaired spin state density is dominant, whereas in other regions where the polarization is entirely due to the self-consistent field (SCF) effect on the wave function, the $m(r)$ may be poorly given and is in general not reliable.

IV. SUMMARY

In this work, we have reported SCF atomic calculations ($Z=3$–$56,79,80$) employing spin-unrestricted OEP and KLI methods within the exchange-only scheme. For comparison, the SUHF and LSDX calculations for the same set of atoms are also performed. Results obtained from these four different schemes are compared.

As is the case for the spin-restricted OEP calculation, the spin-unrestricted OEP yields very similar results as the corresponding SUHF. The total energies deviate from those of the SUHF by at most 40 ppm and diminish with increasing atomic number. Except for a few atoms in the transition series, the OEP and SUHF highest occupied energy eigenvalues corresponding to each spin projection are nearly identical. The electron densities are also close to the SUHF. The expectation values, in particular for those operators which characterize the interior region of the atom, i.e., r^{-1} and $\delta(\mathbf{r})$, agree with SUHF to within a few times 10 ppm or better. The $\langle r^2 \rangle$ value is also in close agreement with the SUHF, with the largest relative difference being only 1%. For most atoms, even the spin density forms a fair approximation to the SUHF. Differences appear to be larger for atoms in the transition group. There are a few cases in the transition series, for which there is a reversal of the order of the state yielding the highest-energy eigenvalue. This result may be partly attributed to the fact that the KS potential always raises the energy levels (relative to SUHF) for the inner shell states. If two states have very small energy difference in the SUHF calculation, such an increase may result in the reversal of the order. In addition, since in exchange-only theory, only the expectation values of the single-particle HF Hamiltonian, $\bar{\varepsilon}_{i\sigma}^{\mathrm{HF}}$, satisfies Koopmans's theorem and that the identity $\varepsilon_{i\sigma}=\bar{\varepsilon}_{i\sigma}^{\mathrm{HF}}$ is true only for the highest $\varepsilon_{i\sigma}$, we thus conclude that the direct OEP calculations may only give the second removal energy and miss the first one (the first one can be calculated by taking the expectation value of the single-particle HF Hamiltonian). Nevertheless, even in this case, the total energy and the electron density of the OEP are still very similar to the corresponding SUHF values. In studying the spin splitting effect, it is found that the OEP and SUHF values are nearly identical for those atoms with the highest occupied states in both spin projections being a p state. Larger disagreements of the OEP and HF spin splitting occur for a few transition elements having an empty $(n-1)d\downarrow$ subshell which demonstrates another noticeable difference of the OEP and SUHF formalisms in describing the s-d interaction. However, as the $(n-1)d\downarrow$ subshell is progressively filled, the large difference is steadily diminished.

The KLI exchange potential possesses many of the analytic properties that the exact KS (OEP) solution obeys and that other approximations lack. It has the capacity of yielding more accurate KS solutions: it gives total energies that are always a significant improvement over those of LSDX; it yields the highest occupied energy eigenvalues of each spin that are very close to those of the OEP or HF; and in most cases, it results in expectation values of $\langle r^2 \rangle$, $\langle r^{-1} \rangle$ (as well as $\langle r \rangle$ and $\langle r^{-2} \rangle$), and $\langle \delta(\mathbf{r}) \rangle$ that are many times more accurate than those of LSDX. For atoms with the highest occupied eigenstate a p state in both spin projections, the KLI spin splitting is also a very accurate approximation to the SUHF or OEP result, having errors of less than 0.6%, whereas that of the LSDX is in error by more than 22%. For atoms with an empty $(n-1)d\downarrow$ subshell, however, the KLI values are significantly in error compared to those of the OEP. For these atoms, the LSDX values may accidentally turn out to be closer, although still having errors larger than 10%. As the $(n-1)d$ subshell is progressively filled, the KLI values once again become closer to those of the OEP as are the latter in approaching those of the SUHF. Like the OEP, there are also cases in the KLI calculations where there is a reversal of the order of the state which yields highest eigenvalue corresponding to a spin projection. From previous analysis, however, this does not form an obstacle in its application. The total energy, the electron density, and the removal energies can all still be very accurately calculated by using the KLI method. Noticeable failure for this approximation is its inability to yield accurate estimates for the spin density at the nucleus for many of the atoms with unpaired p or d electrons. However, most of these atoms have very small $m(0)$ values in exchange-only calculations. In comparing with experiment, the SUHF results are also significantly in error since it is the effect of correlation which plays the most important role for these atoms. In addition, away from the nucleus, in regions where the unpaired p or d state density is dominating, the KLI result still forms a reasonable, and is in general an improved, approximation to the OEP than is the LSDX.

In view of the fact that the KLI method is a very accurate approximation to the exact KS, and is much simpler to employ than the OEP, we expect to find its broad application in the future once accurate, possibly orbital dependent, expressions for the correlation energy functional are developed.

ACKNOWLEDGMENTS

This research was supported by computing resources provided by the City University of New York, University Computer Center. One of us (J.B.K.) acknowledges financial support from the PSC-CUNY research program of the City University of New York.

---

[1] W. Kohn and L. J. Sham, Phys. Rev. **140**, A1133 (1965).

[2] J. P. Perdew and A. Zunger, Phys. Rev. B **23**, 5048 (1981), and references therein.

[3] U. von Barth and L. Hedin, J. Phys. C **5**, 1629 (1972).

[4] J. P. Perdew, R. G. Parr, M. Levy, and J. L. Balduz, Jr., Phys. Rev. Lett. **49**, 1691 (1982).

[5] J. P. Perdew and M. Levy, Phys. Rev. Lett. **51**, 1884 (1983).

[6] L. J. Sham and M. Schluter, Phys. Rev. Lett. **51**, 1888 (1983).

[7] R. T. Sharp and G. K. Horton, Phys. Rev. **90**, 317 (1953).

[8] J. D. Talman and W. F. Shadwick, Phys. Rev. A **14**, 36 (1976).

[9] M. R. Norman and D. D. Koelling, Phys. Rev. B **30**, 5530 (1984).

[10] J. B. Krieger, Y. Li, and G. J. Iafrate, Phys. Lett. A **146**, 256 (1990).

[11] J. B. Krieger, Y. Li, and G. J. Iafrate, Int. J. Quantum Chem. **41**, 489 (1992).

[12] J. B. Krieger, Y. Li, and G. J. Iafrate, Phys. Rev. A **45**, 101 (1992).

[13] Y. Li, J. B. Krieger, and G. J. Iafrate, Chem. Phys. Lett. **191**, 38 (1992).

[14] M. K. Harbola and V. Sahni, Phys. Rev. Lett. **62**, 489 (1989).

[15] Y. Li, J. B. Krieger, M. R. Norman, and G. J. Iafrate, Phys. Rev. B **44**, 10437 (1992). The SICLSD exchange-correlation energy functional is employed in these calculations and the OEP calculations are performed as well. The OEP and KLI results are very similar to each other and they are also quite close to the corresponding SICLSD calculations; see R. A. Heaton, J. G. Harrison, and C. C. Lin, Solid State Commun. **41**, 827 (1982); Phys. Rev. B **28**, 5992 (1983); and M. R. Norman and J. P. Perdew, *ibid.* **28**, 2135 (1983).

[16] S. B. Trickey and J. P. Worth, Int. J. Quantum Chem. Symp. **11**, 529 (1977).

[17] M. Boring, Int. J. Quantum Chem. Symp. **8**, 451 (1974).

[18] U. Roessler, in *Rare Gas Solids,* edited by M. L. Klein and J. A. Venables (Academic, New York, 1975), pp. 505 and 545.

[19] F.-J. Himpsel and W. Steinmann, Phys. Rev. B **17**, 2537 (1978).

[20] T. Koopmans, Physica **1**, 104 (1933).

[21] J. D. Talman, Comput. Phys. Commun. **54**, 85 (1989).

[22] K. Aashamar, T. M. Luke, and J. D. Talman, At. Data Nucl. Data Tables **22**, 443 (1978).

[23] Y. Wang, J. P. Perdew, J. A. Chevary, L. D. Macdonald, and S. H. Vosko, Phys. Rev. A **41**, 78 (1990).

[24] J. B. Krieger, Y. Li, and G. J. Iafrate, Phys. Lett. A **148**, 470 (1990).

[25] M. Levy and J. P. Perdew, Phys. Rev. A **32**, 2010 (1985).

[26] V. Sahni and M. Levy, Phys. Rev. B **33**, 3869 (1986).

[27] Y. Li, J. B. Krieger, J. A. Chevary, and S. H. Vosko, Phys. Rev. A **43**, 5121 (1991).

[28] J. C. Slater, Phys. Rev. **81**, 385 (1951).

[29] See *Handbook of Chemistry and Physics,* 58th ed. (CRC, West Palm Beach, FL, 1978).

[30] P. S. Bagus, B. Liu, and H. F. Schaefer III, Phys. Rev. A **2**, 555 (1970).